Third Harmonic Current Injection in Fault-Tolerant Five-Phase Permanent-Magnet Motor Drive

Guohai Liu, *Senior Member, IEEE*, Zhipeng Lin, Wenxiang Zhao, *Senior Member, IEEE*, Qian Chen, *Member, IEEE*, and Gaohong Xu

***Abstract*—This paper presents a third harmonic current injection method for a five-phase permanent-magnet (PM) motor with trapezoidal back electromotive force (EMF) under postfault field oriented control (FOC). The key of the proposed method is the third harmonic current online calculation and injection under postfault FOC. The postfault FOC lies in the fundamental decoupled model based on the concept of maintaining spatial circular rotation of fundamental PM flux linkage vector and magnetic motive force under open-circuit fault. Based on the mathematical model of torque pulsations caused by third harmonics of air-gap flux, the injected third harmonic current can be calculated by the radio of the amplitude of third harmonic EMF and fundamental EMF easily. The presented fault-tolerant control strategy can achieve the real time optimal current reference generation and third harmonic current injection under postfault FOC while reducing the torque pulsations. The effectiveness of the proposed method is verified by experimental results under various operation conditions.**

***Index Terms*—Decoupled fault model, five-phase permanent-magnet (PM) motor, harmonic current injection, postfault field oriented control (FOC), torque.**

I. Introduction

COMPARED to conventional three-phase machines, multiphase machines offer additional degrees of freedom and can achieve the fault-tolerant operation without any additional hardware [1], [2]. Three-phase machines need using zero-sequence current to maintain the rotating magnetic motive force (MMF), so a neutral line is needed to connect the motor neutral and dc-link midpoint [3], [4]. Multiphase machines can preserve the value of MMF equal to the healthy condition by the existing control technique [5].

Manuscript received June 17, 2017; accepted October 3, 2017. Date of publication October 11, 2017; date of current version April 20, 2018. This work was supported in part by the National Natural Science Foundation of China under Grant 51577084 and Grant 51707083, in part by the Key Project of Natural Science Foundation of Jiangsu Higher Education Institutions under Grant 15KJA470002, in part by the Natural Science Foundation of Jiangsu Province under Grant BK20160518, in part by the Postgraduate Research & Practice Innovation Program of Jiangsu Province under Grant KYCX17_1782, and in part by the Priority Academic Program Development of Jiangsu Higher Education Institutions. Recommended for publication by Associate Editor L. Dalessandro. *(Corresponding Author: Wenxiang Zhao.)*

The authors are with the School of Electrical and Information Engineering, Jiangsu University, Zhenjiang 212013, China, and also with the Jiangsu Key Laboratory of Drive and Intelligent Control for Electric Vehicle, Zhenjiang 212013, China (e-mail: ghliu@ujs.edu.cn; 1044845346@qq.com.cn; zwx@ujs.edu.cn; chenqian0501@ujs.edu.cn; xugaohongujs@163.com.cn).

Color versions of one or more of the figures in this paper are available online at http://ieeexplore.ieee.org.

Digital Object Identifier 10.1109/TPEL.2017.2762320

Open-circuit faults of stator windings and power converter are the most common fault type, which occurs in electrical motors [6]. Many techniques of fault detection and fault tolerant control have been reported. In [7] and [8], an open switch fault detection scheme in voltage–source inverter supplying a permanent-magnet (PM) machine was presented, which was based on the model identification of the motor phase currents. A novel centroid-based diagnostic method of the power switches in five-leg voltage source inverter was presented in [9].

During fault-tolerant operation of multiphase machines, the remaining phase currents have to be rearranged and adapted for open-circuit conditions [5], [10]–[14]. The common criterion of the postfault current reconfiguration is to keep the fundamental MMF same as in the healthy case. Also, by applying additional constraints such as minimum cooper losses, equal cooper losses, and minimum torque ripples, more optimal solutions can be found [5], [10], [11]. Based on the mathematical model of postfault five-phase PM machine, Zhou *et al.* [12] presented a new orthogonal reduced order transformation matrix derived from the fault-tolerant current references and a new zero-sequence current related to torque ripple to achieve postfault field oriented control (FOC) under single phase open-circuit fault. However, the previously discussed solutions can be applied to five-phase machines with sinusoidal stator MMF distribution. They are not applicable to the five-phase PM machine with a trapezoidal back electromotive force (EMF) [13]. The interaction between the high-order harmonic of MMF and fundamental fault-tolerant currents calculated by above methods will produce torque pulsations under open-circuit fault. Tian *et al.* [14] and [15] presented the decoupled models of a five-phase PM machine under single-phase and double-phase open fault, which were used to achieve postfault FOC. The fundamental decoupled models can keep the fundamental torque at d–q frame as the same as the healthy case; however, the third harmonic of winding density distribution results in torque ripple. The sliding mode control was employed to reduce the torque ripples, which can reduce dependency on mathematical model of torque ripples. However, it will cause system chattering and is more difficult to design than PI controller.

Harmonic current injection is the common solution to reduce the torque pulsations produced by the high-order harmonic of MMF [16]–[20], [22]. In [16], the second-order harmonic currents were injected to compensate for nonideal sinusoidal back EMF of tolerant flux-switching PM brushless motor, which can achieve the torque ripple minimization under open-circuit fault.

In order to reduce the torque pulsations caused by the third air-gap flux of five-phase PM motor, the third harmonic current injection techniques were presented in [17]–[20] and [22]. In [17], the fundamental and third harmonic currents were injected in healthy stator phases to increase the average output torque while reducing the torque pulsations, and the healthy currents should present mirror symmetry with respect to the location of the faulty phases. Mohammadpour *et al.* [18]–[20] extended the approach, as mentioned in [17], to different winding configurations under open-circuit and short-circuit faults. In this method, the offline Lagrange algorithms were used to generate optimal reference currents. Lagrange algorithms are part of deterministic algorithms that are based on the gradient computation and it may fail on a local minimum. In optimal current calculation methods based on Lagrange algorithm, the partial derivative of the function f (containing all the objectives to minimize and all constraints) is performed. There is no guarantee that the solution is a global minimum of the problem [21]. In [22], an online optimal current reference generation technique based on vectorial approach was presented for phase open-circuit fault.

Tracking the current reference generation techniques are quite challenging in fault tolerant control. Hysteresis current control is typically employed for current controls [16]–[22]. However, it results in variable switching, which increases switching loss and electromagnetic interference emission [23]. Proportional resonant controller is another solution to tracking time-varying signals [7], [8], which is suitable for operation around a fixed fundamental frequency. In variable-speed drives, however, the fundamental frequency of motor currents is speed dependent. Analysis of transient response of resonant controller for variable-speed drive application was performed in [24] only for a narrow range of frequency (30–50 Hz). However, fundamental frequency varies over a wide range especially in multipole PM machine. In addition, the standard proportional resonant controllers are not suitable for operation near the inverter modulation limit due to their inherently high open loop gain, which may cause stability problem under voltage saturation [25].

In this paper, a fundamental decoupled model of five-phase PM motors under open-circuit faults will be proposed. By maintaining spatial circular rotation of fundamental PM flux linkage vector and MMF, the reduced order Clarke and Park transformations under fundamental rotating space for fault conditions are derived. Thus, FOC and carrier-based PWM can be performed in postfault operation. The fundamental fault-tolerant currents can be calculated with coordinate transformation under $i_d = 0$ control. The torque produced by the fundamental tolerant currents and fundamental PM flux linkages is kept equal to the torque in normal operation. However, the second-order and fourth-order torque pulsations will be produced due to the interaction of the third space air-gap flux linkages and the fundamental fault-tolerant currents. To reduce torque pulsations, a third harmonic current injection method is developed. By this method, the injected third harmonic current can be calculated by the ratio of the amplitude of the third harmonic EMF and fundamental EMF easily based on the mathematical model of torque pulsations. Hence, the real time optimal current reference generation and third harmonic current injection can be achieved under the postfault FOC while reducing the torque pulsations.

The organization of this paper is as follows. The fundamental decoupled modeling and third harmonic current injection under single-phase open-circuit fault is detailed in Section II, and under double-phase open-circuit fault is detailed in Section III. Finally experimental results are provided as confirmation of the effectiveness of the proposed postfault control.

II. Single-Phase Open-Circuit Fault-Tolerant Control

The studied five-phase PM motor with trapezoidal back EMF is fed by a five-phase half-bridge power inverter. In the following discussion, it is assumed that an open-circuit fault has occurred in phase A, and that PM flux density is not affected by the temperature, cogging, and magnetic saturation effects.

A. Decoupled Modeling Under Fundamental Space

In the presence of open fault, the symmetry property of synchronous frame motor model is vanished. For the implementation of FOC under faulty conditions, a new set of Clarke and Park transformations should be developed [14]. The decoupled modeling is based on maintaining spatial circular rotation of fundamental PM flux linkage vector and MMF, and it is described as follows.

Since fundamental MMF is preserved equal to normal mode, for disturbance-free operation the postfault currents can be reconfigured by

$$\frac{5}{2}NI_m e^{\mathrm{j}\left(\theta_e+\pi/2\right)} = N\left(i_A + \alpha i_B + \alpha^2 i_C + \alpha^3 i_D + \alpha^4 i_E\right)$$
$$i_A \equiv 0 \tag{1}$$

where N is winding turns number, I_m is the magnitude of fundamental excitation current, $\alpha = e^{\mathrm{j}\delta}$, δ is the spatial shifting angle between adjacent phases, $\delta = 2\pi/5$, θ_e denotes the rotor electrical position, and i_A, i_B, i_C, i_D, i_E are phase currents.

Since the open-circuit fault has occurred in phase A, the elements about phase A in Clarke transformation matrix should be removed. Since the third row vector is not orthogonal with other row vectors, by removing the third line and correcting the first row vector with zero-sequence current, it can be obtained as

$$\frac{2}{5}\begin{bmatrix} \cos\delta + x & \cos 2\delta + x & \cos 3\delta + x & \cos 4\delta + x \\ \sin\delta & \sin 2\delta & \sin 3\delta & \sin 4\delta \\ \sin 3\delta & \sin 6\delta & \sin 9\delta & \sin 12\delta \\ 1 & 1 & 1 & 1 \end{bmatrix}\begin{bmatrix} i_B \\ i_C \\ i_D \\ i_E \end{bmatrix} = \begin{bmatrix} i_{\alpha 1} \\ i_{\beta 1} \\ i_{31} \\ i_{01} \end{bmatrix} \tag{2}$$

where $i_{\alpha 1}$, $i_{\beta 1}$ are the fundamental space currents at $\alpha - \beta$ plane, respectively, i_{31} represents the third space current, i_{01} is the zero-sequence current, which is constrained to zero because of stator winding star connections, and x is the correction

factor. It should be noted that equality of the first row still holds because of no zero-sequence current.

For postfault operation, the trajectory of fundamental MMFs of healthy phases should also form a circle, and the correction factor x in (2) is selected for above purpose. Thus, a reduced order Clarke transformation is defined as

$$T^A_{\text{Clarke1}} = \frac{2}{5} \times \begin{bmatrix} \cos\delta + x & \cos 2\delta + x & \cos 3\delta + x & \cos 4\delta + x \\ \sin\delta & \sin 2\delta & \sin 3\delta & \sin 4\delta \\ \sin 3\delta & \sin 6\delta & \sin 9\delta & \sin 12\delta \\ 1 & 1 & 1 & 1 \end{bmatrix} \quad (3)$$

where T^A_{clark1} represents the fundamental reduced order Clarke transformation suitable for fault of phase A open-circuit.

Projecting fundamental MMFs of remaining phases to α–β plane with this new reduced order Clarke transformation as

$$\begin{aligned} \psi_{\alpha 1} &= \cos\delta\psi_{B1} + \cos 2\delta\psi_{C1} + \cos 3\delta\psi_{D1} + \cos 4\delta\psi_{E1} \\ &\quad - x\left(\psi_{B1} + \psi_{C1} + \psi_{D1} + \psi_{E1}\right) \\ &= x\psi_{A1} + \cos\delta\psi_{B1} + \cos 2\delta\psi_{C1} + \cos 3\delta\psi_{D1} \\ &\quad + \cos 4\delta\psi_{E1} \end{aligned} \quad (4)$$

$$\psi_{\beta 1} = \sin\delta\psi_{B1} + \sin 2\delta\psi_{C1} + \sin 3\delta\psi_{D1} + \sin 4\delta\psi_{E1} \quad (5)$$

where $\psi_{\alpha 1}$, $\psi_{\beta 1}$ are fundamental MMFs of α–β frame, respectively, and ψ_{A1}, ψ_{B1}, ψ_{C1}, ψ_{D1}, ψ_{E1} are fundamental MMFs at natural reference frame.

Since $\psi_{A1} + \psi_{B1} + \psi_{C1} + \psi_{D1} + \psi_{E1} = 0$, the trajectory of $\psi_{\alpha 1}$ and $\psi_{\beta 1}$ under faulty conditions can form a circle by letting $x = -1$.

The fundamental reduced order Park transformation matrix under single phase open fault can be defined as

$$T^1_{\text{Park1}} = \begin{bmatrix} \cos\theta_e & \sin\theta_e & 0 & 0 \\ -\sin\theta_e & \cos\theta_e & 0 & 0 \\ 0 & 0 & 1 & 0 \\ 0 & 0 & 0 & 1 \end{bmatrix}. \quad (6)$$

Then, with the fundamental reduced order Clarke and Park transformation, as expressed in (3) and (6), the faulty motor model can be transformed into fundamental synchronous frame (d–q–3–0 frame) as

$$\begin{bmatrix} i_{d1} & i_{q1} & i_{31} & i_{01} \end{bmatrix}^T = T^1_{\text{Park1}} T^A_{\text{Clarke1}} \begin{bmatrix} i_B & i_C & i_D & i_E \end{bmatrix}^T. \quad (7)$$

By taking a derivative of magnetic coenergy with respect to rotor mechanical position (θ_m), torque equation can be obtained as

$$T_e = \frac{\partial W_{\text{co}}}{\partial \theta_m} = P\left(\frac{1}{2} I_s^{\text{T}} \frac{\partial L_s}{\partial \theta_e} I_s + I_s^T \frac{\partial \psi_{m-s}}{\partial \theta_e}\right) \quad (8)$$

where W_{co} indicates magnetic coenergy, P is number of pole pairs, I_s represents the phase current vector, L_s indicates phase inductance matrix, ψ_{m-s} represents the vector of PM flux linkages.

In a five-phase motor, the windings are usually wound in a trapezoidal function and give a trapezoidal-shape back EMF. To simplify the postfault modeling, only the first and third harmonics are considered. Since the back-EMFs are produced by the magnetic flux linkages, the PM flux linkages under phase A open-circuit condition are given by

$$\psi^A_{m-s} = \psi_{m1} \begin{bmatrix} \cos(\theta_e - \delta) \\ \cos(\theta_e - 2\delta) \\ \cos(\theta_e - 3\delta) \\ \cos(\theta_e - 4\delta) \end{bmatrix} + \psi_{m3} \begin{bmatrix} \cos 3(\theta_e - \delta) \\ \cos 3(\theta_e - 2\delta) \\ \cos 3(\theta_e - 3\delta) \\ \cos 3(\theta_e - 4\delta) \end{bmatrix} \quad (9)$$

where ψ_{m1} and ψ_{m3} denote, respectively, amplitudes of first and third harmonics of PM flux linkage.

Substitute (3), (6), and (9) into (8), the electromagnetic torque is obtained as follows:

$$T_{e1st} = T_{e1} + T_{e3} \quad (10)$$

$$T_{e1} = \frac{5}{2} P\left[i_{q1}\psi_{m1} + i_{d1} i_{q1}\left(L_d - L_q\right)\right] \quad (11)$$

$$T_{e_3} = \frac{5}{2} P\psi_{m3}\left[3i_{31}\cos 3\theta_e + \frac{3i_{d1}\left(\sin 2\theta_e + \sin 4\theta_e\right)}{2} + \frac{3i_{q1}\left(-\cos 2\theta_e + \cos 4\theta_e\right)}{2}\right] \quad (12)$$

where T_{e1st} denotes overall electromagnetic torque produced by fundamental currents, T_{e1} is the fundamental torque, and T_{e3} stands for ripples in the torque, produced by the fundamental currents and third air-gap flux linkages.

B. Postfault FOC Under Fundamental Space

According to (10), the average value of postfault torque is determined by the fundamental torque (T_{e1}). Clearly, with $i_d = 0$ control the average torque can be determine by i_{q1}. The third space current value (i_{31}) can be acquired by imposing additional constraints: fundamental phase current reconfiguration is calculated by lowest joule losses (LJL) or equal joule losses (EJL) control criteria.

1) LJL Control Criterion: Since the joule loss can be expressed by $R_s(i_{d1}^2 + i_{q1}^2 + i_{31}^2)$, where i_{q1} is constant, it is clear that minimal loss is achieved by adopting $i_{d1} = 0$ and $i_{31} = 0$ control. The current references of d–q–3 frame can be presented as

$$i_{d1} = 0 \;\; i_{q1} = i_{\text{qr}}, \;\; i_{31} = 0. \quad (13)$$

2) EJL Control Criterion: When the EJL criterion is adopted, the current amplitude of each healthy phase is required to be kept equal. In this case, the healthy currents can be reconfigured by imposing extra constraint of $i_B = -i_D$ and $i_C = -i_E$. Substitute this constraint into (2), the following relationship can be obtained as:

$$\begin{aligned} i_{\beta 1} &= \sin\delta i_B + \sin 2\delta i_C + \sin 3\delta i_D + \sin 4\delta i_E \\ &= \left(i_B + i_C\right)\left(\sin\delta + \sin 2\delta\right) \end{aligned} \quad (14)$$

$$\begin{aligned} i_{31} &= \sin 3\delta i_B + \sin 6\delta i_C + \sin 9\delta i_D + \sin 12\delta i_E \\ &= \frac{\sin\delta - \sin 2\delta}{\sin\delta + \sin 2\delta} i_{\beta 1} = 0.236 i_{q1}\cos\theta_e. \end{aligned} \quad (15)$$

The reference current of d–q–3 frame for the purpose of EJL control can be presented as

$$i_{d1}=0 \;\; i_{q1}=i_{qr} \;\; i_{31}=0.236 i_{q1}\cos\theta_e. \tag{16}$$

Substitute (13) and (16) into (10), the torque (T_{e1}) produced by fundamental current can be kept equal to the prefault rated torque. The torque ripples (T_{e3}) concentrates mainly on the frequency that is twice and four times synchronous speed. To reduce the second-order and fourth-order torque pulsations, the third harmonic current can be injected strategically.

C. Third Harmonic Current Injection

In third harmonic space, the same method can be used to get the third harmonic decoupled modeling. The principle is to maintain the third harmonic MMF and back-EMF the same as in normal operation. Duplicating the method in fundamental space, the reduced order Clarke and Park transformations matrix under third harmonic space can be defined as

$$T^{A}_{\text{Clarke3}}=\frac{2}{5}\times\begin{bmatrix}\sin\delta & \sin 2\delta & \sin 3\delta & \sin 4\delta\\ \cos 3\delta+x & \cos 6\delta+x & \cos 9\delta+x & \cos 12\delta+x\\ \sin 3\delta & \sin 6\delta & \sin 9\delta & \sin 12\delta\\ 1 & 1 & 1 & 1\end{bmatrix} \tag{17}$$

$$T^{1}_{\text{Park3}}=\begin{bmatrix}1 & 0 & 0 & 0\\ 0 & \cos 3\theta_e & \sin 3\theta_e & 0\\ 0 & -\sin 3\theta_e & \cos 3\theta_e & 0\\ 0 & 0 & 0 & 1\end{bmatrix} \tag{18}$$

where T^{A}_{clark3} represents the third harmonic reduced order Clarke transformation under phase A open-circuit. T^{1}_{Park3} represents the third harmonic reduced order Park transformation under single-phase open-circuit fault.

Then, with the reduced order Clarke and Park transformation under third harmonic space, as expressed in (17) and (18), the faulty motor model can be transformed into third harmonic synchronous frame (3–d–q–0 frame) as

$$\begin{bmatrix} i_{33} & i_{d3} & i_{q3} & i_{03}\end{bmatrix}^T = T^{1}_{\text{Park3}}T^{A}_{\text{Clarke3}}\begin{bmatrix} i_B & i_C & i_D & i_E\end{bmatrix}^T \tag{19}$$

where i_{d3}, i_{q3} are third harmonic space currents at d–q plane, respectively; i_{33} is the generalized zero-sequence current; and i_{03} is the zero-sequence current, which is constrained to zero.

Substitute (17), (18), and (9) into (8), the electromagnetic torque produced by third harmonic current is obtained as

$$T_{e3\text{rd}}=\frac{5P}{2}\left\{3\psi_{m3}i_{q3}+\psi_{m1}\left[\frac{i_{d3}(\sin 4\theta_e-\sin 2\theta_e)}{2}+\frac{i_{q3}(\cos 4\theta_e-\cos 2\theta_e)}{2}\right]+i_{33}\cos\theta_e\right\}. \tag{20}$$

According to the superposition principle, the electromagnetic torque produced by fundamental and third harmonic currents can obtain as $T_e=T_{e1\text{st}}+T_{e3\text{rd}}$. The components of T_e at different frequency can be presented as

$$\begin{cases}\tau_0=\frac{5P}{2}\left(\psi_{m1}i_{q1}+3\psi_{m3}i_{q3}\right)\\ \tau_1=\frac{5P}{2}\psi_{m1}i_{33}\cos\theta_e\\ \tau_2=\frac{5P}{4}\left[3\psi_{m3}\left(i_{d1}\sin 2\theta_e-i_{q1}\cos 2\theta_e\right)\right.\\ \qquad\left.-\psi_{m1}\left(i_{d3}\sin 2\theta_e+i_{q3}\cos 2\theta_e\right)\right]\\ \tau_3=\frac{5P}{2}3\psi_{m3}i_{31}\cos 3\theta_e\\ \tau_4=\frac{5P}{4}\left[3\psi_{m3}\left(i_{d1}\sin 4\theta_e+i_{q1}\cos 4\theta_e\right)\right.\\ \qquad\left.+\psi_{m1}\left(i_{d3}\sin 4\theta_e+i_{q3}\cos 4\theta_e\right)\right]\end{cases} \tag{21}$$

where τ_0 is the average torque component, τ_1, τ_2, τ_3, and τ_4 represent the fundamental, second-order, third-order, and fourth-order torque pulsation, respectively.

When the current quantities of d–q axis satisfy the following relationship represented as (22), the second-order and fourth-order torque pulsations can be eliminated

$$\begin{cases}i_{d1}=i_{d3}=0\\ i_{q3}=-\dfrac{3\psi_{m3}}{\psi_{m1}}i_{q1}=-k_{psi}i_{q1} \quad k_{psi}=\dfrac{3\psi_{m3}}{\psi_{m1}}=\dfrac{E_3}{E_1}\end{cases} \tag{22}$$

where k_{psi} is the ratio of the amplitude of the third harmonic EMF, (E_3), and fundamental EMF, (E_1).

The i_{31} and i_{33} can be acquired by imposing additional constraints.

1) LJL Control Criterion: Since the joule losses produced by third harmonic current can be expressed by $R_s(i^2_{d3}+i^2_{q3}+i^2_{33})$, it is clear that total minimal losses value $R_s(i^2_{q1}+i^2_{q3})$ is achieved by the following relationship:

$$i_{31}=0, \;\; i_{33}=0. \tag{23}$$

Since the $i_{31}=0$ and $i_{33}=0$, the torque pulsations at different frequency in (21) can be constrained to zero.

2) EJL Control Criterion: When the EJL criterion $(i_{31}=0.236 i_{q1}\cos\theta_e)$ is adopted, the torque pulsation τ_1 is not zero. However, the $\tau_1+\tau_3$ can be constrained to zero by choosing the appropriate value of i_{33}. i_{31} and i_{33} should satisfy the following relationship:

$$i_{31}=0.236 i_{q1}\cos\theta_e, \quad i_{33}=0.236 i_{q3}\cos 3\theta_e. \tag{24}$$

Adopting third harmonic current injection, torque pulsation free operation under single-phase open fault condition can be achieved.

III. Double-Phase Open-Circuit Fault-Tolerant Control

In a five-phase machine, two different types of double-phase fault may occur, i.e., open fault of two adjacent or nonadjacent phases. The principle for decoupled modeling under above two fault conditions is similar, and the derivation method is similar to that of single-phase open-circuit.

A. Fundamental Decoupled Model

Assume that double-phase open-circuit fault happens in a five-phase motor, healthy phase currents should be reconfigured to maintain equal MMF before and after fault operation. On the

other hand, the trajectory of MMFs of healthy phases should also form a circle. Based on above two principles, the Clarke and Park transformations under double-phase open-circuit can be redefined [15].

The fundamental reduced order Clarke transformation matrix under two adjacent phases (phase A and B open-circuit) is redefined as (25) shown at the bottom of this page.

The fundamental reduced order Park transformation matrix under double-phase open-circuit can be redefined as

$$T^2_{\mathrm{Park1}} = \begin{bmatrix} \cos\theta_e & \sin\theta_e & 0 \\ -\sin\theta_e & \cos\theta_e & 0 \\ 0 & 0 & 1 \end{bmatrix}. \tag{26}$$

With the Clarke and Park transformation under phase A and B open-circuit, the faulty motor model can be transformed into fundamental synchronous frame (d–q–0 frame), and the motor fundamental phase current can be expressed as

$$\begin{bmatrix} i_{d1} & i_{q1} & i_{01} \end{bmatrix}^T = T^2_{\mathrm{Park1}} T^{AB}_{\mathrm{Clarke1}} \begin{bmatrix} i_C & i_D & i_E \end{bmatrix}^T \tag{27}$$

where i_{d1}, i_{q1} are the fundamental currents at d–q plane, respectively; i_{01} is the zero-sequence current, which is constrained to zero because of stator winding star connections.

Under open-circuit of phase A and B, the PM flux linkages are presented as

$$\psi^{AB}_{m-s} = \psi_{m1} \begin{bmatrix} \cos(\theta_e - 2\delta) \\ \cos(\theta_e - 3\delta) \\ \cos(\theta_e - 4\delta) \end{bmatrix} + \psi_{m3} \begin{bmatrix} \cos 3(\theta_e - 2\delta) \\ \cos 3(\theta_e - 3\delta) \\ \cos 3(\theta_e - 4\delta) \end{bmatrix}. \tag{28}$$

With proposed coordinate transformation, the fundamental phase current solutions for $i_d = 0$ control under open-circuit of phase A and B are shown by

$$\begin{aligned} \begin{bmatrix} i_{C1} \\ i_{D1} \\ i_{E1} \end{bmatrix} &= \left[T^{AB}_{\mathrm{Clarke1}}\right]^{-1} \left[T^2_{\mathrm{Park1}}\right]^{-1} \begin{bmatrix} i_{d1} \\ i_{q1} \\ 0 \end{bmatrix} \\ &= \begin{bmatrix} -2.236 i_{q1} \sin(\theta_e - \frac{2\pi}{5}) \\ 3.618 i_{q1} \sin(\theta_e - \frac{\pi}{5}) \\ -2.236 i_{q1} \sin\theta_e \end{bmatrix}, \quad i_{d1} \equiv 0. \end{aligned} \tag{29}$$

Substitute (28) and (29) to (8), the electromagnetic torque produced by fundamental fault-tolerant current under open-circuit of phase A and B is obtained as

$$\begin{aligned} T^{AB}_{e1\mathrm{st}} = \frac{5P i_{q1}\psi_{m1}}{2} \Bigg[1 + \frac{3\psi_{m3}}{\psi_{m1}} \cos(2\theta_e - \delta) \\ + \frac{4.845\psi_{m3}}{\psi_{m1}} \cos(4\theta_e + \frac{\delta}{2}) \Bigg]. \end{aligned} \tag{30}$$

Similarly, the fundamental reduced order Clarke transformation matrix under two nonadjacent phases (phase A and C open-circuit) can be redefined as (31) shown at the bottom of this page.

The motor fundamental phase current under phase A and C open-circuit at d–q–0 frame can be expressed by

$$\begin{bmatrix} i_{d1} & i_{q1} & i_{01} \end{bmatrix}^T = T^2_{\mathrm{Park1}} T^{\mathrm{AC}}_{\mathrm{Clarke1}} \begin{bmatrix} i_B & i_D & i_E \end{bmatrix}^T. \tag{32}$$

Under open-circuit of phase A and C, the PM flux linkages are presented as

$$\psi^{AC}_{m-s} = \psi_{m1} \begin{bmatrix} \cos(\theta_e - \delta) \\ \cos(\theta_e - 3\delta) \\ \cos(\theta_e - 4\delta) \end{bmatrix} + \psi_{m3} \begin{bmatrix} \cos 3(\theta_e - \delta) \\ \cos 3(\theta_e - 3\delta) \\ \cos 3(\theta_e - 4\delta) \end{bmatrix}. \tag{33}$$

With proposed coordinate transformation, fundamental phase current solutions for $i_d = 0$ control under open-circuit of phase A and C are shown by

$$\begin{aligned} \begin{bmatrix} i_{B1} \\ i_{D1} \\ i_{E1} \end{bmatrix} &= \left[T^{\mathrm{AC}}_{\mathrm{Clarke1}}\right]^{-1} \left[T^2_{\mathrm{Park1}}\right]^{-1} \begin{bmatrix} i_{d1} \\ i_{q1} \\ 0 \end{bmatrix} \\ &= \begin{bmatrix} -1.382 i_{q1} \sin(\theta_e - \frac{2\pi}{5}) \\ 2.236 i_{q1} \sin\theta_e \\ -2.236 i_{q1} \sin(\theta_e + \frac{\pi}{5}) \end{bmatrix}, \quad i_{d1} \equiv 0. \end{aligned} \tag{34}$$

Substitute (33) and (34) to (8), the electromagnetic torque produced by fundamental fault-tolerant current under open-circuit of phase A and C is obtained as

$$\begin{aligned} T^{\mathrm{AC}}_{e1\mathrm{st}} = \frac{5P i_{q1}\psi_{m1}}{2} \Bigg[1 + \frac{3\psi_{m3}}{\psi_{m1}} \cos(2\theta_e - 2\delta) \\ + \frac{1.854\psi_{m3}}{\psi_{m1}} \cos(4\theta_e + \delta) \Bigg], \quad i_{d1} \equiv 0. \end{aligned} \tag{35}$$

As can been seen from expressions (30) and (35), the average electromagnetic torque produced by fundamental fault-tolerant current can remain the same as normal operation. However,

$$T^{AB}_{\mathrm{Clarke1}} = \frac{2}{5} \begin{bmatrix} \cos 2\delta - \cos\delta & \cos 3\delta - \cos\delta & \cos 4\delta - \cos\delta \\ \sin 2\delta - \tan\frac{\delta}{2}\cos\delta & \sin 3\delta - \tan\frac{\delta}{2}\cos\delta & \sin 4\delta - \tan\frac{\delta}{2}\cos\delta \\ 1 & 1 & 1 \end{bmatrix} \tag{25}$$

$$T^{\mathrm{AC}}_{\mathrm{Clarke1}} = \frac{2}{5} \begin{bmatrix} \cos\delta - \cos 2\delta & \cos 3\delta - \cos 2\delta & \cos 4\delta - \cos 2\delta \\ \sin\delta - \tan\delta\cos 2\delta & \sin 3\delta - \tan\delta\cos 2\delta & \sin 4\delta - \tan\delta\cos 2\delta \\ 1 & 1 & 1 \end{bmatrix} \tag{31}$$

due to the third harmonics of air-gap flux, the torque pulsations concentrate mainly on the frequency that is twice and four times synchronous speed. To reduce the second-order and fourth-order torque pulsations, the third-harmonic currents can be injected strategically.

B. Third Harmonic Current Injection

The third harmonic of PM flux linkages interact with fundamental excitation currents, generating the second-order and fourth-order torque pulsations. While the injected third harmonic currents can interact with fundamental PM flux linkages to generate the opposite second-order and fourth-order torque pulsations, in this way, the originally existing torque pulsations can be eliminated.

1) Under Open-Circuit of Phase A and B: Under this fault condition, the injected third harmonic currents can be defined as

$$\begin{cases} i_{C3} = k_1 i_{q1} \sin(3\theta_e + \varphi_1) \\ i_{D3} = k_2 i_{q1} \sin(3\theta_e + \varphi_2) \\ i_{E3} = k_3 i_{q1} \sin(3\theta_e + \varphi_3) \end{cases} \tag{36}$$

where k_1, k_2, k_3 are proportional coefficient of phase currents amplitude, respectively, and φ_1, φ_2, φ_3 are current phases.

Substitute (28) and (36) to (8), the electromagnetic torque produced by third harmonic current can be obtained. The second-order and fourth-order torque pulsations produced by third harmonic current and fundamental PM flux linkage can be factorized as

$$\begin{aligned} T^{AB}_{\mathrm{e3rd(C2)}} &= -\frac{i_{q1}\psi_{m1}\cos(2\theta_e)}{2}\left[k_1\cos(\varphi_1+0.8\pi)\right. \\ &\quad \left.+k_2\cos(\varphi_2-0.8\pi)+k_3\cos(\varphi_3-0.4\pi)\right] \\ T^{AB}_{e\mathrm{3rd(S2)}} &= \frac{i_{q1}\psi_{m1}\sin(2\theta_e)}{2}\left[k_1\sin(\varphi_1+0.8\pi)\right. \\ &\quad \left.+k_2\sin(\varphi_2-0.8\pi)+k_3\sin(\varphi_3-0.4\pi)\right] \\ T^{AB}_{e\mathrm{3rd(C4)}} &= \frac{i_{q1}\psi_{m1}\cos(4\theta_e)}{2}\left[k_1\cos(\varphi_1-0.8\pi)\right. \\ &\quad \left.+k_2\cos(\varphi_2+0.8\pi)+k_3\cos(\varphi_3+0.4\pi)\right] \\ T^{AB}_{e\mathrm{3rd(S4)}} &= -\frac{i_{q1}\psi_{m1}\sin(4\theta_e)}{2}\left[k_1\sin(\varphi_1-0.8\pi)\right. \\ &\quad \left.+k_2\sin(\varphi_2+0.8\pi)+k_3\sin(\varphi_3+0.4\pi)\right] \end{aligned} \tag{37}$$

where $T^{AB}_{\mathrm{e3rd(C2)}}$, $T^{AB}_{e\mathrm{3rd(S2)}}$, $T^{AB}_{e\mathrm{3rd(C4)}}$ $T^{AB}_{e\mathrm{3rd(S4)}}$ represent the cosine and sine component of second-order and fourth-order torque pulsation produced by the third harmonic currents under phase A and B open-circuit fault, respectively.

The torque pulsation of electromagnetic torque (31) can be factorized as

$$\begin{aligned} T^{AB}_{e1st(\mathrm{C2})} &= \frac{5Pi_{q1}}{2}3\psi_{m3}\cos(0.4\pi)\cos(2\theta_e) \\ T^{AB}_{e1st(\mathrm{S2})} &= \frac{5Pi_{q1}}{2}3\psi_{m3}\sin(0.4\pi)\sin(2\theta_e) \end{aligned}$$

TABLE I
MOTOR PARAMETERS

Symbol	Description	Quantity
ψ_{m1}	Fundamental PM flux linkage	0.0411 Wb
ψ_{m3}	third harmonic PM flux linkage	0.0033 Wb
L_d	d-axis inductance	0.9323 mH
L_q	q-axis inductance	1.2614 mH
P	Pole pairs	9
N_{s}	Slot number	20

$$\begin{aligned} T^{AB}_{e1st(\mathrm{C4})} &= \frac{5Pi_{q1}}{2}3\psi_{m3}1.615\cos(0.2\pi)\cos(4\theta_e) \\ T^{AB}_{e1st(\mathrm{S4})} &= -\frac{5Pi_{q1}}{2}3\psi_{m3}1.615\sin(0.2\pi)\sin(4\theta_e) \end{aligned} \tag{38}$$

where $T^{AB}_{e1st(\mathrm{C2})}$, $T^{AB}_{e1st(\mathrm{S2})}$, $T^{AB}_{e1st(\mathrm{C4})}$, $T^{AB}_{e1st(\mathrm{S4})}$ represent the cosine and sine component of second-order and fourth-order torque pulsation produced by the fundamental currents under phase A and B open-circuit fault, respectively.

In order to eliminate the second-order and fourth-order torque pulsations, the above mentioned torque components of (37) and (38) should be constrained to zero. So the following relationships can be obtained as

$$\begin{aligned} &T^{AB}_{e1st(\mathrm{C2})} + T^{AB}_{e3rd(\mathrm{C2})} = 0\ ;\ T^{AB}_{e1st(\mathrm{S2})} + T^{AB}_{e3rd(\mathrm{S2})} = 0 \\ &T^{AB}_{e1st(\mathrm{C4})} + T^{AB}_{e3rd(\mathrm{C4})} = 0\ ;\ T^{AB}_{e1st(\mathrm{S4})} + T^{AB}_{e3rd(\mathrm{S4})} = 0. \end{aligned} \tag{39}$$

Due to the star connections of stator winding, the summation of the third harmonic phase currents should be constrained to zero. The following relationships are established as follows:

$$\begin{aligned} &i_{q1}\cos 3\theta_e\left(k_1\sin\varphi_1 + k_2\sin\varphi_2 + k_3\sin\varphi_3\right) = 0 \\ &i_{q1}\sin 3\theta_e\left(k_1\cos\varphi_1 + k_2\cos\varphi_2 + k_3\cos\varphi_3\right) = 0. \end{aligned} \tag{40}$$

It can be seen that there are six equations (39), (40) to find the solution for the six unknown variables of the third harmonic currents (36). Thus, the unique solution can be found as

$$\begin{cases} i_{C3} = 4.799 k_{psi} i_{q1}\sin(3\theta_e + 4.566) \\ i_{D3} = 9.461 k_{psi} i_{q1}\sin(3\theta_e + 1.257) \\ i_{E3} = 4.799 k_{psi} i_{q1}\sin(3\theta_e + 4.229). \end{cases} \tag{41}$$

The interaction of the third harmonic current and the fundamental MMF can eliminate the second-order and fourth-order torque pulsations. But the above mentioned third harmonic current and the third harmonic MMF also can produce a torque component expressed by

$$T^{AB'}_{e3rd} = -3Pk_{psi}i_{q1}\psi_{m3}\left[9.03 + 8.08\sin(6\theta_e + 0.9436)\right]. \tag{42}$$

It can be observed that the electromagnetic torque (42) produced by third harmonic currents and the third harmonic MMF consists of an average torque component and a sixth-order torque pulsation. The peak to peak torque ripple in (30) accounts for 103.3% (i.e., values of ψ_{m1} and ψ_{m3} are referred to Table I) under just fundamental current injected. After the injection of third harmonic current, the peak to peak torque ripple is reduced to 47.6%.

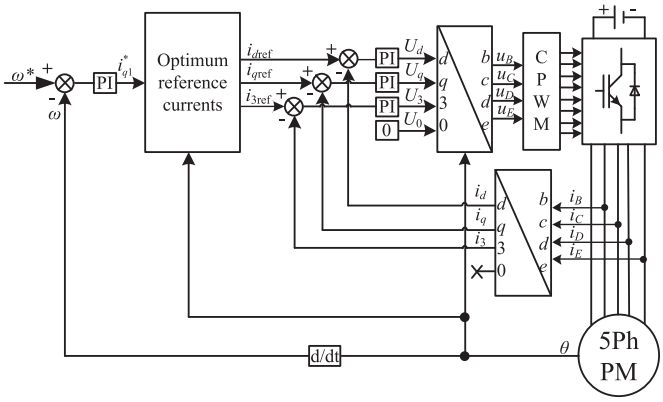

Fig. 1. Overall control scheme under single-phase open-circuit fault.

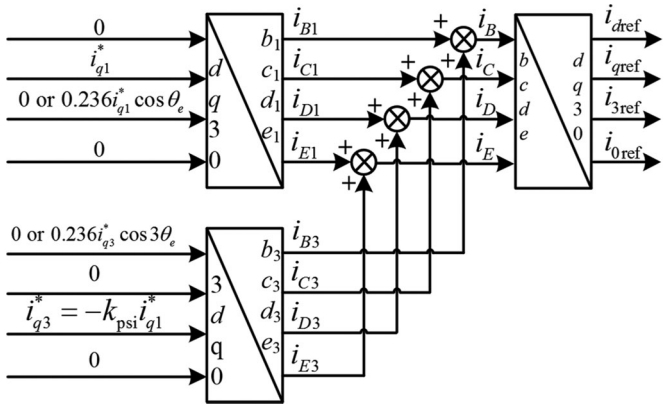

Fig. 2. Schematic of the optimum reference currents under single-phase open-circuit.

2) Under Open-Circuit of Phase A and C: The principle introduced above is also applied to fault condition of phase A and C open-circuit, and the injected third harmonic currents under this fault condition are given by

$$\begin{cases} i_{B3} = 0.528 k_{psi} i_{q1} \sin\left(3\theta_e + 2.513\right) \\ i_{D3} = 3.451 k_{psi} i_{q1} \sin\left(3\theta_e + 0.866\right) \\ i_{E3} = 3.451 k_{psi} i_{q1} \sin\left(3\theta_e + 4.161\right). \end{cases} \tag{43}$$

Similarly, the interaction of the third harmonic current and the fundamental MMF can eliminate the second-order and fourth-order torque pulsations under open-circuit of phase A and C. But the above mentioned third harmonic current and the third harmonic MMF also can produce a torque component expressed by

$$T_{e3rd}^{\mathrm{AC}'} = -3P k_{psi} i_{q1} \psi_{m3} \left[3.46 + 3.09 \sin\left(6\theta_e + 0.314\right)\right]. \tag{44}$$

The electromagnetic torque (44) also consists of an average torque component and a sixth-order torque pulsation. The peak to peak torque ripple in (35) accounts for 58.8% under just fundamental current injected. After the injection of third harmonic current, the peak to peak torque ripple is reduced to 14.4%.

IV. Experimental Verification

A. Control System Configuration

Fig. 1 shows the overall control scheme under single-phase open-circuit fault. The diagram of the optimum reference currents in Fig. 1 is given in Fig. 2, and it is constructed according to the theory introduced above.

The control scheme under double-phase open-circuit fault is similar to single-phase open-circuit fault. In the case of double-phase open-circuit, the d–q–0 frame is used instead of d–q–3–0 frame, so the control variables of third space $i_{3\mathrm{ref}}$, U_3 in Fig. 1 can be removed. Fig. 3 shows the schematic of the optimum reference currents under open fault of phases A and B.

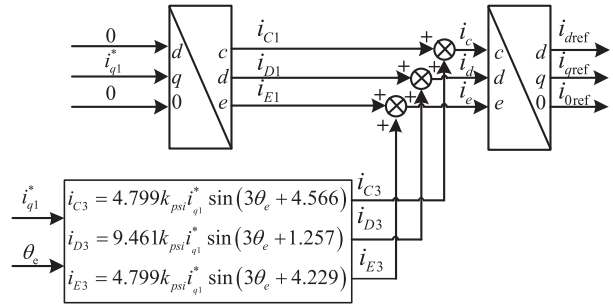

Fig. 3. Schematic of the optimum reference currents under open fault of adjacent phases.

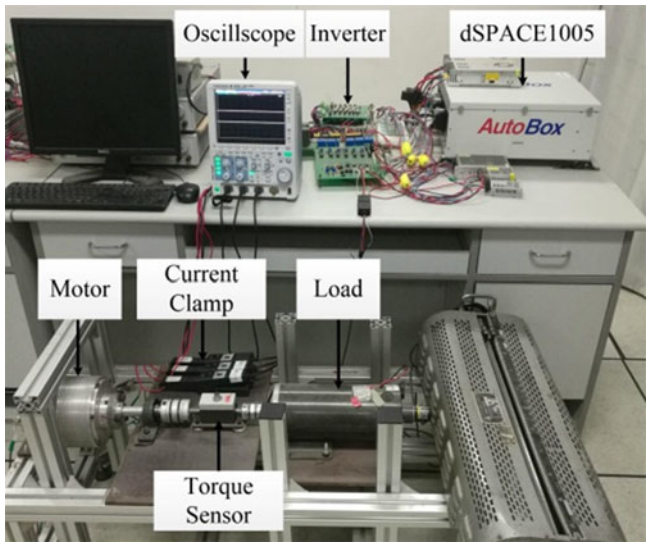

Fig. 4. Experimental test platform.

B. Experimental Measurements

In order to verify the suitability of proposed model and proposed algorithm, a test platform has been set up as shown in Fig. 4. The experiment set is composed of an in-wheel five-phase PM motor, a five-phase half-bridge inverter, and a dc generator as the load. The dSPACE1005 controller is utilized for the implementation of overall control algorithm. Motor parameters are listed in Table I. The motor torque is measured by

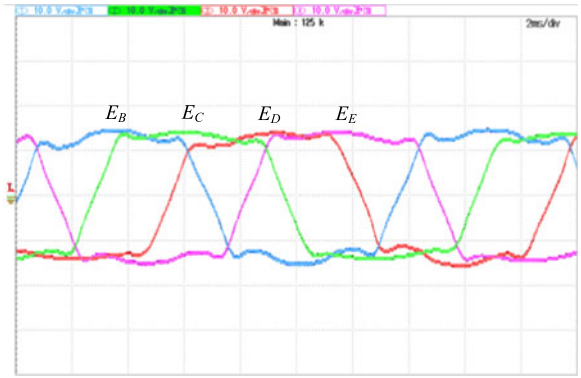

Fig. 5. Back-EMFs of healthy phases; EMFs are scaled to 10 V/div.

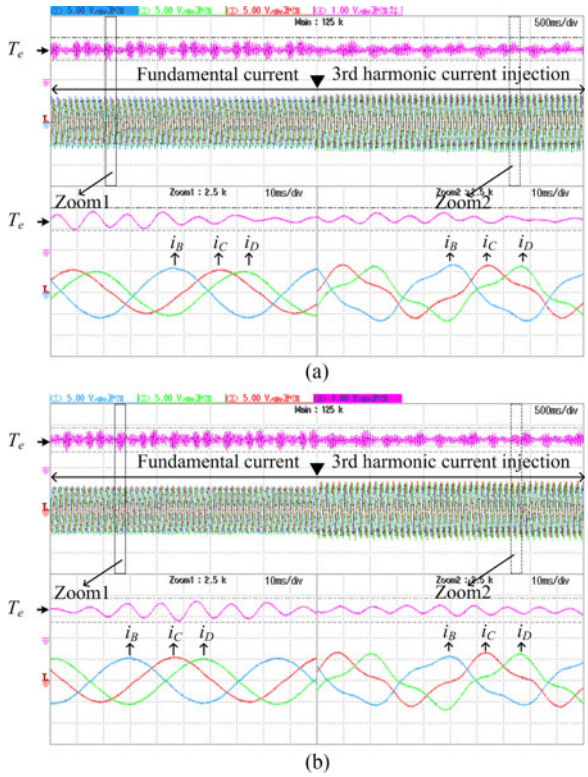

Fig. 6. Torque and currents waveforms before and after third harmonic current injection under open-circuit of phase A using: (a) LJL criterion and (b) EJL criterion. T_e is scaled to 2 N·m/div, and phase currents are scaled to 5 A/div.

a high precision torque transducer (HBM T20WN/20NM). The frequency of IGBTs is fixed at 10 kHz, the sample rate of the current sensor is 10 kHz, and the dc-link voltage is 50 V.

Since the oscilloscope used during the experiment has only four input channels, there are only four back-EMF curves shown in Fig. 5. The fast Fourier transform of the measured back-EMF data is carried out to obtain its frequency components. It is found that the machine back-EMF contains 20% of third harmonic. So the value of k_{psi} used in experiment is 20%.

Fig. 6 shows the torque and phase current waveforms before and after the injection of third harmonic current under respectively LJL and EJL control criteria when phase A is open-circuit. The motor is operated at a constant speed of 120 r/min, and the torque ripple is 53.6% in healthy condition at this speed. LJL

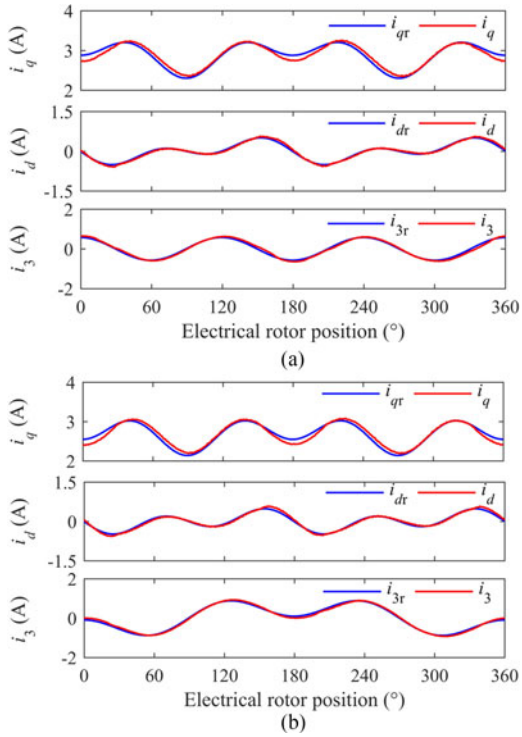

Fig. 7. Waveforms of d–q–3 frame reference and feedback currents after third harmonic current injection under open-circuit of phase A using: (a) LJL criterion and (b) EJL criterion.

control is performed in Fig. 6(a). The torque ripple is 75.9% under the fundamental current and 58.9% under third harmonic current injection. The torque and phase currents under fundamental current and third-harmonic current injection using LJL criterion has been magnified and shown in Zoom1 and Zoom2. In Zoom1, the amplitude of phase B is higher than phase C and D. Fig. 6(b) shows the torque and phase currents, respectively, under fundamental current and third harmonic current injection using EJL criteria. The torque ripple is, respectively, 83.1% and 64.6% before and after third harmonic current injection. The current amplitudes of remaining phases are equal in the Zoom1. From Fig. 6, it can be seen that the torque ripple can be reduced successfully by the presented third harmonic currents injection method under single-phase open-circuit fault.

Fig. 7 shows the reference and feedback d–q–3 currents in an electrical periodic under phase A open-circuit. It should be noted the third harmonic current will be transformed to second and fourth harmonic components by the fundamental reduced order Park transformation, which is the reason why the d–q–3 frame currents in Fig. 7 are not a constant quantity but containing the second and fourth harmonic components. With the same load, the waveforms of the d-axis and q-axis currents under LJL control criteria are the same as the currents under EJL control criteria. The waveforms of i_3 under two control criteria are different. As can be seen from Fig. 7, the d–q–3 frame feedback currents can track the reference currents accurately.

Fig. 8 refers to the torque and healthy phase currents before and after third harmonic currents injection under, respectively, open fault of adjacent and nonadjacent phases. The motor

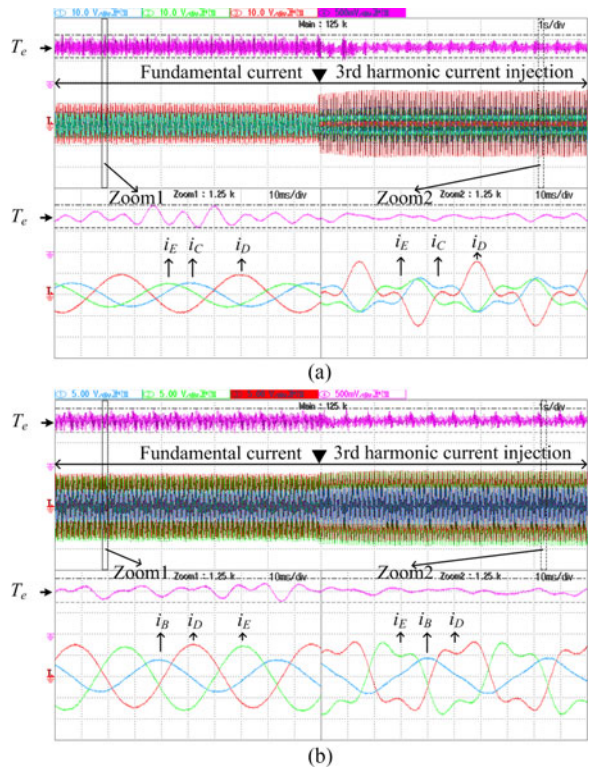

Fig. 8. Torque and currents waveforms before and after third harmonic current injection under: (a) open-circuit of phase A and B and (b) open-circuit of phase A and C. T_e is scaled to 1 N·m/div, and phase currents are scaled to 10 A/div in (a) and 5 A/div in (b).

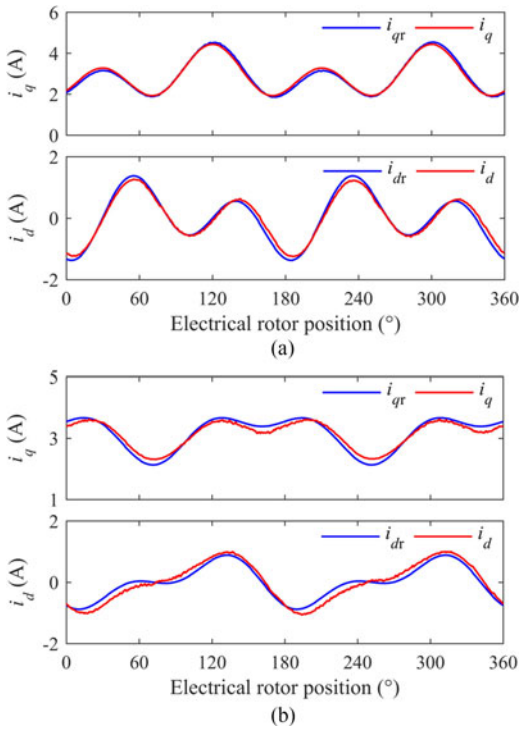

Fig. 9. Waveforms of d–q frame reference and feedback currents after third harmonic current injection under: (a) open-circuit of phases A and B and (b) open-circuit of phases A and C.

operates at a constant speed of 150 r/min. At this speed, the torque ripple is 35.3% under healthy condition. The torque ripple is 65.3% under fundamental current and 43.2% under third harmonic current injection, as shown in Fig. 8(a). In Fig. 8(b), it can be noted that after third harmonic current injection, torque ripples are reduced to 40.6% whereas approximately 58.4% under fundamental current. The magnified torque and healthy currents before and after third harmonic current injection, respectively, are shown in Zoom1 and Zoom2. The amplitude and phase of the measured currents match the theoretical value.

Fig. 9 shows the reference and feedback d–q frame currents after third harmonic current injection under, respectively, open fault of adjacent and nonadjacent phases. The second and fourth harmonic components of the d–q frame currents are used to reduce the second-order and fourth-order torque pulsations. As can be seen from the Fig. 9, the d–q frame feedback currents can track the reference currents successfully.

From above analysis, it can be noted that the torque ripples cancellation is actually accomplished with the presented third harmonic current injection. The proposed control scheme can achieve the third harmonic current injection under postfault FOC.

V. Conclusion

This paper has investigated general postfault control method for a five-phase PM motor with trapezoidal back EMF under open-circuit fault. Decoupled motor models at fundamental synchronous rotating coordinate have been derived under, respectively, single-phase open-circuit and double-phase open-circuit. Based on above models, FOC and carrier-based PWM can be utilized to operate a faulty motor. The fundamental current calculated by the decoupled motor models under fundamental synchronous rotating coordinate can keep the average torque equal to that of healthy condition. Due to the third harmonic PM flux linkages, the second-order and fourth-order torque pulsations emerge, so the online third harmonic current injection methods have been proposed to reduce the second-order and fourth-order torque pulsations. The proposed postfault control method has been experimentally verified, both results demonstrate that the proposed postfault control method can achieve the third harmonic current injection under postfault FOC and torque ripples cancellation successfully.

References

[1] M. Bermudez, I. Gonzalez-Prieto, F. Barrero, H. Guzman, M. J. Duran, and X. Kestelyn, "Open-phase fault-tolerant direct torque control technique for five-phase induction motor drives," *IEEE Trans. Ind. Electron.*, vol. 64, no. 2, pp. 902–911, Sep. 2017.

[2] I. Gonzalez-Prieto, M. J. Duran, and F. J. Barrero, "Fault-tolerant control of six-phase induction motor drives with variable current injection," *IEEE Trans. Power Electron.*, vol. 32, no. 10, pp. 7894–7903, Oct. 2017.

[3] D. Zhou, J. Zhao, and Y. Liu, "Predictive torque control scheme for three-phase four-switch inverter-fed induction motor drives with DC-link voltages offset suppression," *IEEE Trans. Power Electron.*, vol. 30, no. 6, pp. 3309–3318, Jun. 2015.

[4] N. M. A. Freire and A. J. M. Cardoso, "A fault-tolerant PMSG drive for wind turbine applications with minimal increase of the hardware requirements," *IEEE Trans. Ind. Appl.*, vol. 50, no. 3, pp. 2039–2049, May/Jun. 2014.

[5] Q. Chen, G. Liu, W. Zhao, L. Qu, and G. Xu, "Asymmetrical SVPWM fault-tolerant control of five-phase PM brushless motors," *IEEE Trans. Energy Convers.*, vol. 32, no. 1, pp. 12–22, Mar. 2017.
[6] M. J. Duran and F. Barrero, "Recent advances in the design, modeling, and control of multiphase machines—Part II," *IEEE Trans. Ind. Electron.*, vol. 63, no. 1, pp. 459–468, Jan. 2016.
[7] M. Salehifar, R. S. Arashloo, J. M. Moreno-Eguilaz, V. Sala, and L. Romeral, "Observer-based open transistor fault diagnosis and fault-tolerant control of five-phase permanent magnet motor drive for application in electric vehicles," *IET Power Electron.*, vol. 8, no. 1, pp. 76–87, Jan. 2015.
[8] M. Salehifar, R. S. Arashloo, J. M. Moreno-Equilaz, V. Sala, and L. Romeral, "Fault detection and fault tolerant operation of a five phase PM motor drive using adaptive model identification approach," *IEEE J. Emerg. Sel. Topics Power Electron.*, vol. 2, no. 2, pp. 212–223, Jun. 2014.
[9] M. Trabelsi, N. K. Nguyen, and E. Semail, "Real-time switches fault diagnosis based on typical operating characteristics of five-phase permanent-magnetic synchronous machines," *IEEE Trans. Ind. Electron.*, vol. 63, no. 8, pp. 4683–4694, Aug. 2016.
[10] G. Liu, L. Qu, W. Zhao, Q. Chen, and Y. Xie, "Comparison of two SVPWM control strategies of five-phase fault-tolerant permanent-magnet motor," *IEEE Trans. Power Electron.*, vol. 31, no. 9, pp. 6621–6630, Sep. 2016.
[11] H. Guzman *et al.*, "Comparative study of predictive and resonant controllers in fault-tolerant five-phase induction motor drives," *IEEE Trans. Ind. Electron.*, vol. 63, no. 1, pp. 606–617, Jan. 2016.
[12] H. Zhou, W. Zhao, G. Liu, R. Cheng, and Y. Xie, "Remedial field-oriented control of five-phase fault-tolerant permanent-magnet motor by using reduced-order transformation matrices," *IEEE Trans. Ind. Electron.*, vol. 64, no. 1, pp. 169–178, Jan. 2017.
[13] L. Parsa and H. A. Toliyat, "Five-phase permanent-magnet motor drives," *IEEE Trans. Ind. Appl.*, vol. 41, no. 1, pp. 30–37, Jan./Feb. 2005.
[14] B. Tian, Q. T. An, J. D. Duan, D. Y. Sun, L. Sun, and D. Semenov, "Decoupled modeling and nonlinear speed control for five-phase PM motor under single-phase open fault," *IEEE Trans. Power Electron.*, vol. 32, no. 7, pp. 5473–5486, Jul. 2017.
[15] B. Tian, Q. T. An, J. D. Duan, D. Semenov, D. Y. Sun, and L. Sun, "Cancellation of torque ripples with FOC strategy under two-phase failures of the five-phase PM motor," *IEEE Trans. Power Electron.*, vol. 32, no. 7, pp. 5459–5472, Jul. 2017.
[16] W. Zhao, M. Cheng, K. T. Chau, and C. C. Chan, "Control and operation of fault-tolerant flux-switching permanent-magnet motor drive with second harmonic current injection," *IET Elect. Power Appl.*, vol. 6, no. 9, pp. 707–715, Nov. 2012.
[17] S. Dwari and L. Parsa, "Fault-tolerant control of five-phase permanent-magnet motors with trapezoidal back EMF," *IEEE Trans. Ind. Electron.*, vol. 58, no. 2, pp. 476–485, Feb. 2011.
[18] A. Mohammadpour and L. Parsa, "A unified fault-tolerant current control approach for five-phase PM motors with trapezoidal back EMF under different stator winding connections," *IEEE Trans. Power Electron.*, vol. 28, no. 7, pp. 3517–3527, Jul. 2013.
[19] A. Mohammadpour, S. Sadeghi, and L. Parsa, "A generalized fault-tolerant control strategy for five-phase PM motor drives considering star, pentagon, and pentacle connections of stator windings," *IEEE Trans. Ind. Electron.*, vol. 61, no. 1, pp. 63–75, Jan. 2014.
[20] A. Mohammadpour and L. Parsa, "Global fault-tolerant control technique for multiphase permanent-magnet machines," *IEEE Trans. Ind. Appl.*, vol. 51, no. 1, pp. 178–186, Jan./Feb. 2015.
[21] E. B. Sedrine, J. Ojeda, M. Gabsi, and I. Slama-Belkhodja, "Fault-tolerant control using the GA optimization considering the reluctance torque of a five-phase flux switching machine," *IEEE Trans. Energy Convers.*, vol. 30, no. 3, pp. 927–938, Sep. 2015.
[22] X. Kestelyn and E. Semail, "A vectorial approach for generation of optimal current references for multiphase permanent-magnet synchronous machines in real time," *IEEE Trans. Ind. Electron.*, vol. 58, no. 11, pp. 5057–5065, Nov. 2011.
[23] B. Sen and J. Wang, "Stationary frame fault-tolerant current control of polyphase permanent-magnet machines under open-circuit and short-circuit faults," *IEEE Trans. Power Electron.*, vol. 31, no. 7, pp. 4684–4696, Jul. 2016.
[24] A. G. Yepes, A. Vidal, F. D. Freijedo, J. Malvar, O. Lopez, and J. Doval-Gandoy, "Transient response evaluation of resonant controllers for AC drives," in *Proc. 2012 IEEE Energy Convers. Congr. Expo.*, 2012, pp. 471–478.
[25] S. A. Richter and R. W. De Doncker, "Digital proportional-resonant (PR) control with anti-windup applied to a voltage-source inverter," in *Proc. 14th Eur. Conf. Power Electron. Appl.*, 2011, pp. 1–10.

Guohai Liu (M'07–SM'15) received the B.Sc. degree from Jiangsu University, Zhenjiang, China, in 1985, and the M.Sc. and Ph.D. degrees from Southeast University, Nanjing, China, in 1988 and 2002, respectively, all in electrical engineering and control engineering.

Since 1988, he has been with Jiangsu University, Zhenjiang, where he is currently a Professor, and the Dean of the School of Electrical Information Engineering. From 2003 to 2004, he was a Visiting Professor in the Department of Electronic and Electrical Engineering, University of Sheffield, Sheffield, U.K. His teaching and research interests include electrical machines, motor drives for electric vehicles, and intelligent control. He has authored or coauthored more than 200 technical papers and four textbooks, and holds 30 patents in these areas.

Zhipeng Lin received the B.Sc. degree in control engineering from Jiangsu University, Zhenjiang, China, in 2016, where he is currently working toward the M.Sc. degree in control science and engineering.

His current research interests include power-electric control of electric machines and fault tolerant control.

Wenxiang Zhao (M'08–SM'14) received the B.Sc. and M.Sc. degrees in electrical engineering from Jiangsu University, Zhenjiang, China, in 1999 and 2003, respectively, and the Ph.D. degree in electrical engineering from Southeast University, Nanjing, China, in 2010.

Since 2003, he has been with Jiangsu University, Zhenjiang, where he is currently a Professor in the School of Electrical Information Engineering. From 2008 to 2009, he was a Research Assistant in the Department of Electrical and Electronic Engineering, University of Hong Kong, Hong Kong. From 2013 to 2014, he was a Visiting Professor in the Department of Electronic and Electrical Engineering, University of Sheffield, Sheffield, U.K. His current research interests include electric machine design, modeling, fault analysis, and intelligent control. He has authored and coauthored more than 130 technical papers in these areas.

Qian Chen (M'16) received the B.Sc. and Ph.D. degrees from Jiangsu University, Zhenjiang, China, in 2009 and 2015, respectively, both in electrical engineering and control engineering.

Since 2015, he has been with Jiangsu University, Zhenjiang, where he is currently a Lecturer in the School of Electrical Information Engineering. His current research interests include electric machine design, modeling, fault analysis, and intelligent control.

Gaohong Xu received the B.Sc. and M.Sc. degrees from Jiangsu University, Zhenjiang, China, in 2009 and 2011, respectively. She is currently working toward the Ph.D. degree in Jiangsu University, Zhenjiang.

Her current research interests include computation of electromagnetic fields for permanent-magnet machine, and electric machine design.